PRAMANA — journal of physics
© Indian Academy of Sciences
Vol. 79, No. 1
July 2012
pp. 113–124

Main reaction process simulation of hydrogen gas discharge in a cold cathode electric vacuum device

JING-YE LIU, YUAN GAO* and GANG WANG
School of Science, Beijing University of Chemical Technology, Beijing, 100029, China
*Corresponding author. E-mail: gaoyuan25526@163.com

MS received 8 May 2011; revised 1 February 2012; accepted 8 February 2012

Abstract. Based on the related theory of plasma discharge process and the COMSOL multi-physics software, and considering the corresponding boundary conditions, the related reaction types in the hydrogen plasma discharge were simulated and analysed, and the main reactions of hydrogen discharge in small electric vacuum components at low pressure and weak ionization were confirmed. Among the 21 types of reactions in hydrogen discharge process, 11 of them play important roles under low pressure and weak ionization in cold cathode electric vacuum device. The simulated results are consistent with the test result.

Keywords. Plasma discharge; reactions; hydrogen; collision; process simulation.

PACS Nos 52.65.−y; 52.75.Kq; 52.20.Fs

1. Introduction

The research on cold-cathode weakly-ionized plasma glow discharge is important in the field of gas discharge. In the cold-cathode weakly-ionized gas discharge, the main reason for the plasma gas discharge is the collision reactions in the gas. Therefore, it is very significant in basic research as well as in actual applications.

In the low-pressure weakly-ionized plasma discharge research, researchers pay more attention to the inert gas discharge collision reactions [1–4] whereas the study on hydrogen discharge reaction is rare. Furthermore, because of the peculiarity of the structure of hydrogen molecules, as an electric vacuum switch device working gas, hydrogen molecules has same advantages over inert gas. Therefore, the research on hydrogen discharge collision reactions is of great significance.

Generally, according to the study of Yoon *et al* [5], there are 21 types of collision reactions in hydrogen discharge, and a reliable cross-section data of collision process in the hydrogen discharge are obtained. But, when low-pressure weakly-ionized cold cathode electric vacuum device is studied, it is seen that not all these 21 collision reactions play leading roles in the hydrogen gas discharge. In this paper, it is based on the model of

DOI: 10.1007/s12043-012-0292-7; ***e*Publication: 25 May 2012**

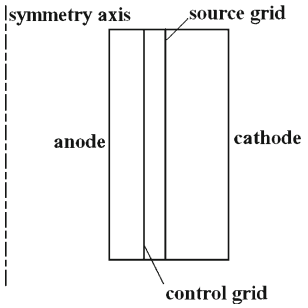

Figure 1. Schematic drawing of the model structure.

axisymmetric cylindrical switching device. Figure 1 shows the two-dimensional simplified cut-away view, which includes the cathode (radius = 31 mm), source grid (radius = 22 mm), control grid (radius = 18.5 mm) and anode (radius = 14 mm). The impact of 21 types of reactions in the hydrogen discharge was analysed and discussed in detail, and the finite element method was used to simulate and corroborate. Finally, the main types of hydrogen discharge reactions at low pressure and weak ionization are found. The necessary theoretical reference for cold cathode electric vacuum device research is provided.

2. Theoretical analysis

According to [5–8], there are five categories of correlation reactions in hydrogen plasma which are excitation, de-excitation, ionization, attachment and elastic collision reactions. Under the five reaction categories, there are 21 kinds of reactions, which include electron–neutral molecule reaction, ion–neutral molecule reaction, neutral–neutral molecule reaction, wall combination and so on [9]. In the cold cathode electric vacuum device, under low pressure and weak ionization, elastic collision reaction is encountered by most electrons, that is, $e + H_2 \rightarrow H_2 + e$ and $e + H \rightarrow H + e$, but the inelastic collision is the key method for ionizing the working gas and constituting plasma [10].

The inelastic collision has four categories, such as excitation, de-excitation, ionization and attachment reactions. The main reactions of hydrogen plasma formed in the switching device are discussed below.

2.1 *Excitation and de-excitation*

When electronic energy is 8.8 eV, the hydrogen molecule is excited to the repellent state $b^3\Sigma_u^+$, and then it is decomposed to two higher energy hydrogen atoms (average energy of each atom is approximately 2.2 eV), that is, $e + H_2 \rightarrow e + 2H$ [9].

When electronic energy reaches 11.5 eV, the molecule can be excited to the second excited state $B^1\Sigma_u^+$ [11], ($e + H_2 \rightarrow H_2^* + e$), then electric dipole radiation occurs in ultraviolet band and the molecule will return to the ground state. That is, hydrogen molecules in the excited states radioactively decay to the ground level [12].

When electronic energy reaches 11.8 eV, hydrogen molecule can be stimulated to the bound states $E, F^1\Sigma_g^+$, then electric dipole reaches the repellent state, decomposes and produces higher hydrogen atoms (average energy of each atom is approximately 2.2 eV). The final reaction will be $e + H_2 \rightarrow 2H + e$ [11].

When electronic energy reaches 12.6 eV, the hydrogen molecule can be excited to the state $C^1\Pi_u$, undergo the reaction $e + H_2 \rightarrow e + H_2^* + h\mu$, and return to the ground state after emitting ultraviolet photon [12].

De-excitation reactions can be regarded as the counter-reaction of excitation, a process that transforms the atoms in the excited state to the ground state due to some reasons such as emission of photons [13]. Along with the above four excitation reactions, de-excitation reactions are also present.

2.2 *Ionization*

When the molecules continue to receive energy from outside, and the energy is large enough, ionization occurs. When the electronic energy reaches 13.6 eV, hydrogen atoms in the system can ionize and the reaction is $e + H \rightarrow 2e + H^+$. When the electron energy reaches 15.4 eV, the hydrogen molecules began to ionize [11]. Then they will produce H_2^+ ions, and the reaction process is $e + H_2 \rightarrow 2e + H_2^+$.

When the electronic energy reaches 18.1 eV, electrolysis occurs, $e + H_2 \rightarrow 2e + H + H^+$, with the production of H and H^+ whose energies are about 5 eV [5].

When the electrons are excited, dissociation threshold energy of H_2 will be 847 kJ/mol (8.8 eV), ionization threshold energy of H_2 will be 1483 kJ/mol (15.4 eV) and ionization threshold energy of H will be 1310 kJ/mol (13.6 eV). When the plasma system is under the pressure of tens to several thousands Pa, the dissociation rate is about an order of magnitude larger than the ionization rate. Considering the energy, in the case of medium energy input, hydrogen atoms may be the primary dissociation particles in the non-equilibrium weakly ionized hydrogen plasma [13]. In addition, when H_2 generates H^+, it needs larger energy. Compared with H_2, H has a smaller ionization cross-section [9] and so H_2^+ concentration is greater than H^+ concentration. Therefore, the main ionization reaction is, $e + H_2 \rightarrow 2e + H_2^+$.

2.3 *Attachment reaction*

With ionization reaction occurs in the system, attachment reaction also occurs. Considering the model studied in this paper, the main attachment reaction is the reaction between electrons and ions. Hydrogen plasma basically has hydrogen atoms, hydrogen molecules and hydrogen ions (H^+, H_2^+, H_3^+) [14]. Although the electrons have some affinity to hydrogen atoms and molecules, in the low-pressure non-equilibrium state plasma, it will not produce anions due to electronic adsorption, such as H_2^-, because electronic energy cannot reach the energy of the thermion (about 40 eV above). Therefore, there are no

attachment reactions for positive ions and anions. The attachment reactions considered in this paper are mainly the following [9]:

$$e + H^+ \rightarrow H,$$

$$e + H_2^+ \rightarrow H_2$$

$$e + H_3^+ \rightarrow H_2 + H.$$

Among these three reactions, the reaction $e + H_2^+ \rightarrow H_2$ is the most important. The main ions in the plasma system are determined by the reactions between ions and neutral molecules. H^+ and H_2^+ react with H_2 and produce H_3^+ [6]. The velocity of these reactions increases as the density of the hydrogen molecule increases. According to the state equation $pV = nRT$, the gas volume V and the operating temperature T are constant, R is the molar gas constant, the amount of hydrogen molecules increases with the gas pressure, while the density of hydrogen molecule increases with the gas pressure. However, when the gas pressure is more than 665 Pa (5 torr), it is difficult to detect H_3^+ in the plasma [13]. Even if H_3^+ exists, when electrons and H_3^+ attachment reaction occurs, it needs more than 11.75 eV energy, but very few electrons can achieve this energy. Therefore, the reactions are not dominating [7]. Also, high energy is needed to produce positive ions (H_3^+, H_2^+, H^+). Compared to H_2^+, H has smaller ionization cross-section, and the concentration of H^+ is far less than H_2^+ [6,13]. So the attachment reaction between electrons and H_2^+ plays a leading role in the switching device.

3. Simulation and confirmation

According to the theoretical analysis discussed earlier, since H_2 has a bigger ionization cross-section than H in low-pressure and weakly-ionized hydrogen plasma, two attachment reactions where H is produced is ignored, and only the reaction $e + H_2^+ \rightarrow H_2$ is considered. While, five kinds of reaction types that H_3^+ existed, the ionization reaction that generated H^+, the elastic collision and attachment reactions, totally eight kinds of reactions should be discussed in this paper.

The geometric model is given in figure 1. Compared with the inert gas discharge characteristics, the hydrogen plasma discharge properties are summarized using the DC discharge model in plasma module. Finally, considering the reaction types and the species of the particles, combining with the electric neutrality of plasma, each reaction type in the system is simulated and analysed, to confirm the main reaction of the working process in the whole switching devices. The pressure is 1 torr and the temperatures is 293.15 K.

3.1 *Simulation calculation theory*

$$\frac{\partial n_e}{\partial t} + \nabla \cdot \Gamma_e = R_e - (\vec{u} \cdot \nabla) n_e, \tag{1}$$

$$\Gamma_e = -(\mu_e \cdot \vec{E}) n_e - D_e \cdot \nabla n_e, \tag{2}$$

$$\frac{\partial n_\varepsilon}{\partial t} + \nabla \cdot \Gamma_\varepsilon + \vec{E} \cdot \Gamma_\mathrm{e} = S_\mathrm{en} - (\vec{u} \cdot \nabla)\, n_\varepsilon + \frac{(Q + Q_\mathrm{gen})}{q}, \tag{3}$$

$$\Gamma_\varepsilon = -(\mu_\mathrm{en} \cdot \vec{E}) n_\varepsilon - D_\mathrm{en} \cdot \nabla n_\varepsilon, \tag{4}$$

$$\vec{E} = -\nabla V, \tag{5}$$

$$\nabla \cdot \vec{D} = \rho_\mathrm{v}, \tag{6}$$

$$-\vec{n} \cdot (\vec{D}_1 - \vec{D}_2) = \rho_\mathrm{s}, \tag{7}$$

in which

$$D_\mathrm{e} = \mu_\mathrm{e} T_\mathrm{e}, \quad \mu_\mathrm{en} = \frac{5}{3}\mu_\mathrm{e}, \quad D_\mathrm{en} = \mu_\mathrm{en} T_\mathrm{e}.$$

Equation (1) is the electron density continuity equation, eq. (2) is the electron flux expression, eq. (3) is the electronic energy density continuous equation, eq. (4) is the electronic energy flux expression and eq. (7) is the boundary conditions. Here, n_e is the electron density, Γ_e is the electron flux, R_e is the net production rate of the electrons, $\vec{u}$ is the electronic speed, μ_e is the electron mobility, $\vec{E}$ is the electric intensity, D_e is the electronic diffusion coefficient, n_ε is the electronic energy density, Γ_ε is the electronic energy flux, S_en is the source of electronic energy, D_en is the electronic energy diffusion coefficient, μ_en is the electronic energy mobility, Q is the heat generated by induced current or electromagnetic wave, that is inductive power or microwave power, Q_gen represents the total heat, that is the total power, $\vec{D}$ is the electric displacement vector, ρ_v is the volume charge density, ρ_s is the surface charge density, T_e is the electron temperature.

3.2 *Exclusion of correlation response about the H_3^+ ions produced*

As discussed above, there are 21 reactions in pure hydrogen plasma. But by theoretical analysis, when pressure is low ($P < 0.133$ Pa), we can eliminate the existence of H_3^+; the reaction between H_3^+ and neutral molecules does not exist. And because the wall recombination reaction is related to H_3^+ ions, this surface reaction will not happen. From the simulation result, one can make out that for all the reactions where H_3^+ exists, whether as a reactant or as a product, the calculation results are not convergent. It is indicated that all the reactions associated with H_3^+ in cold cathode electric vacuum device did not happen.

3.3 *The analysis of $e + H_2 \rightarrow 2e + H + H^+$ reaction*

In the following, the ionization reaction in which H^+ ions are produced will be discussed. As we know, when electronic energy reaches 15.4 eV, collision ionization reactions occur,

electronic energy continues to increase, and when it reaches 18.1 eV or higher, the reaction $e + H_2 \rightarrow 2e + H + H^+$ will occur. This reaction is one of the main reaction that needs to be discussed.

In the simulation analysis we discovered that if the reaction $e + H_2 \rightarrow 2e + H + H^+$ exists in the process, no matter how other parameters change, the electron and ion concentration distributions can be drawn in the following relation curves.

In the figures, the horizontal axis shows the distance from the source grid to the cathode, the vertical axis shows ion density, solid line stands for electronic concentrations distribution, dotted line is for H_2^+ concentration distribution and dash–dot line expresses H^+ concentration. Figures 2 to 5 show the relationship of electron and ion concentrations with time when the ionization reaction $e+H_2 \rightarrow 2e+H+H^+$ exists. The graph shows that electron density n_e is not equal to ion density n_i when steady-state is reached. Although the concentrations of the electrons and the ions have the same order of magnitude, it can

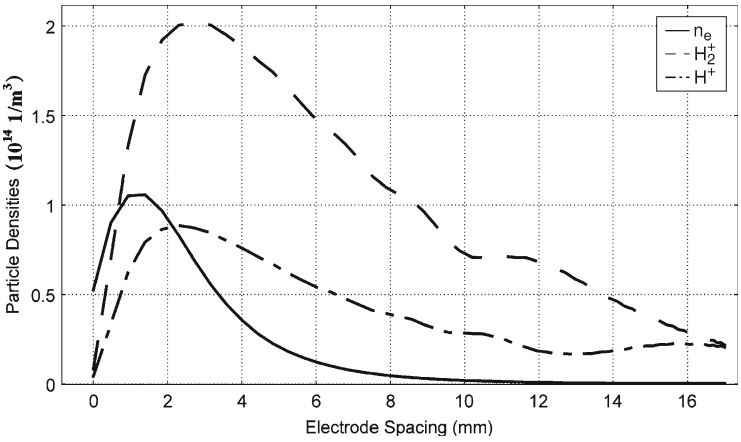

Figure 2. Electron and ion concentration distributions at 3.63e−7s.

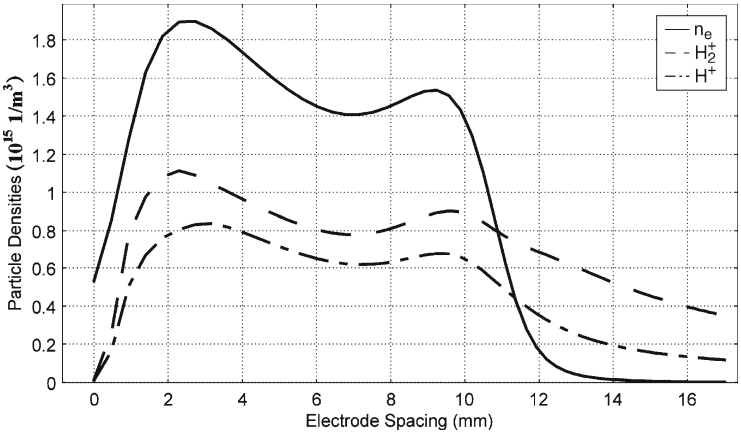

Figure 3. Electron and ion concentration distributions at 8.31e−7s.

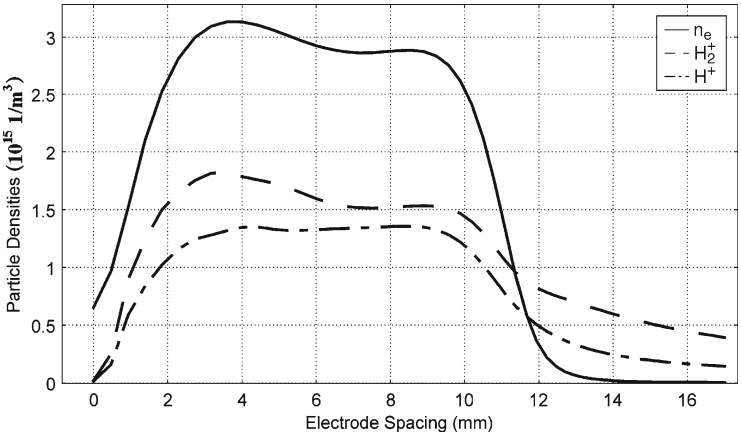

Figure 4. Electron and ion concentration distributions at 1.45e−6s.

be seen from the graphs that electron concentration is about half of the ion concentration at 3.63e − 7s. With the further occurrence of the reaction, the electronic energy increases gradually under the influence of the electric field, electrons collide with the gas molecules constantly, and then generate new electrons. At the same time, positive ions move to the cathode slowly, and when the positive ions reach the cathode, they collide with the cathode and release secondary electrons. In the entire reaction, there will still be collision and ionization of electron and neutral molecules, but this rate is more than the rate in which positive ions are produced and thus, with the advancement of the process, the electron concentration will increase, and at 6.31e − 7s, the electron concentration is about twice that of the ion concentration, which means that in the device, it does not reach electric neutrality, but reaches electronegativity condition [15]. In theory [11], it should satisfy the relationship $n_i = n_e$ in the steady-state plasma. But now in the existing collision ionization reaction process that we have discussed, it would break the steady-state criteria.

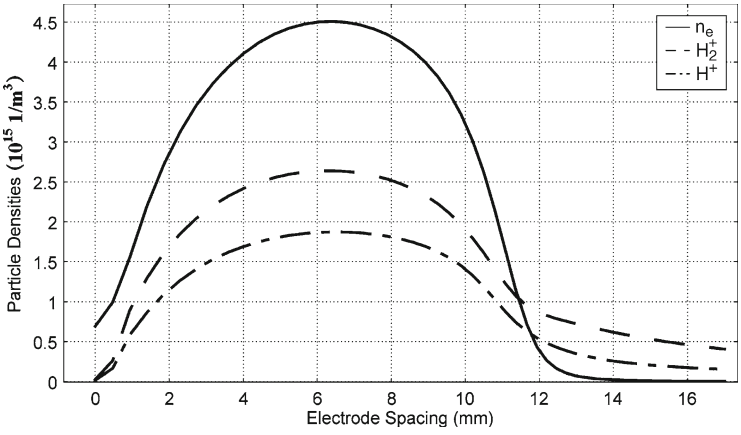

Figure 5. Electron and ion concentration distributions at 1e−5s.

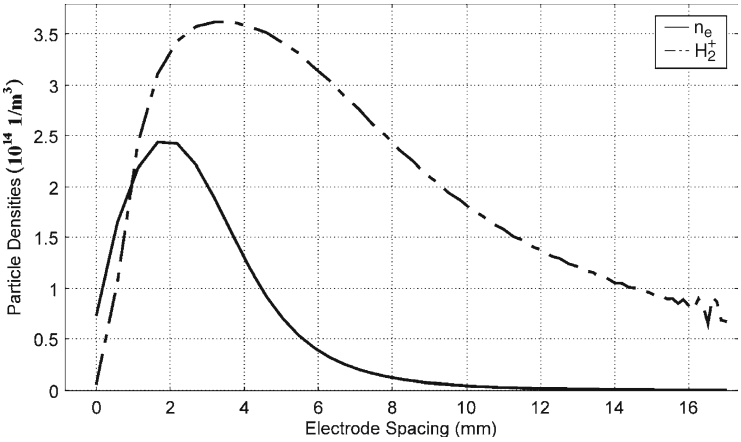

Figure 6. Electron and ion concentration distributions at 8.31e−7s.

Therefore, $e+H_2 \rightarrow 2e+H+H^+$ reaction does not exist, for the reaction process is not physically correct in weakly-ionized low-pressure plasma.

Figures 6 to 8 are electron and ion distribution curves after excluding the reaction $e+H_2 \rightarrow 2e+H+H^+$. Both ends of the device are the anode and the cathode. From the figures we can see that because of the effect of the electric field, electrons move to the anode promptly, its concentration increases gradually near the anode, then it spreads to the cathode surface until it reaches the cathode sheath. At 1e − 6s, the system achieves electric neutrality state. As shown in figure 8, as the time increases, the system achieves steady state.

Figure 9 shows the potential distribution at different moments in the system after eliminating the reaction $e+H_2 \rightarrow 2e+H+H^+$. Here it is shown that the plasma is basically

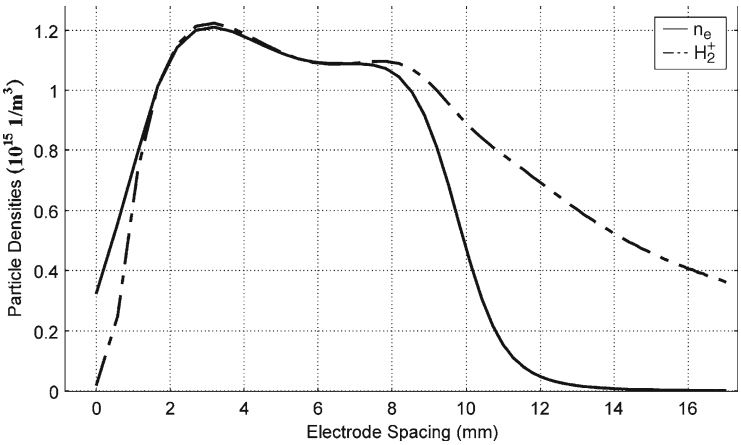

Figure 7. Electron and ion concentration distributions at 1.45e−6s.

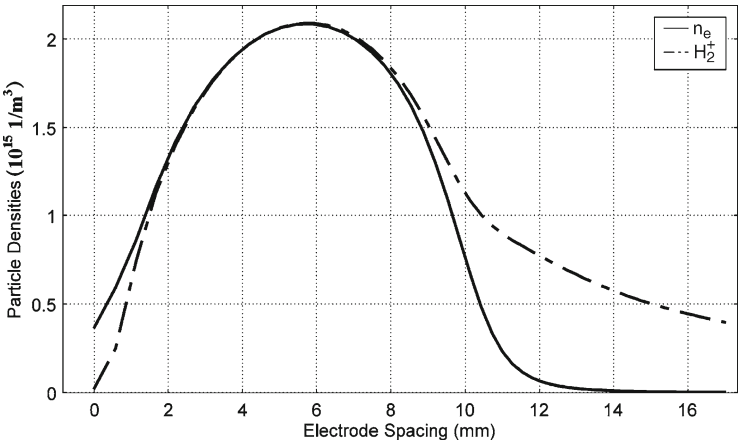

Figure 8. Electron and ion concentration distributions at 1e−5s.

formed at 6.3e − 7s, and as the time increases the potential curve tends towards zero, and the plasma system achieves dynamic balance. Judging by the potential distribution curve at 9e − 5s, the rapid potential changes in the sheath near the cathode (in the horizontal axis 16–12 mm), and voltage drop mainly occur in this region. As the electrons and ions move to a dynamic equilibrium, the cathode potential relative to the potential of the main plasma is negative. In this figure 10–12 mm area is called the neutral zone, and this area is the transition region where the electrons within the sheath penetrate the main plasma area. It has a small potential with the main plasma area, and ions accelerate to the cathode. The 0–6 mm area is the main plasma area, and in this area the electron concentration is equal to the ion concentration, the slope of the potential curve is zero, and the electric intensity is zero [15].

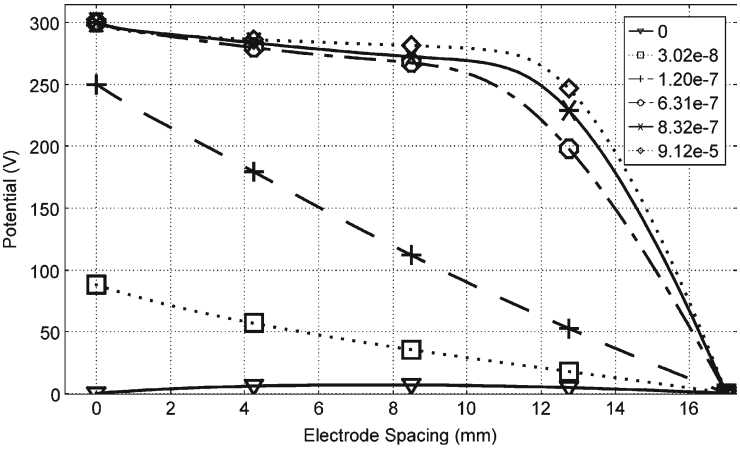

Figure 9. The potential distribution during plasma formation.

Above all, there is no $e+H_2 \rightarrow 2e+H+H^+$ reaction. As a result of excluding the reaction that electrons collide with hydrogen molecule and produce H^+, there are no $H^+ \rightarrow H_2$ reactions on the electrode surface. It will not be considered as an influence in the device.

3.4 *The elastic collision reaction*

The $e+H \rightarrow H+e$ reaction can be ignored in low-pressure weakly-ionized plasma. Based on the related theory, when the electron energy is small, atoms cannot be exciting or ionizing at the collision process of electrons and hydrogen atoms, because compared to the hydrogen atoms the electrons' mass is quite small, after collision electron energy has no loss basically. In addition, as H atom has a smaller ionization cross-section, the chances for the collision between electrons and H atoms are much smaller than the chances for collisions between electrons and hydrogen molecules and so can be ignored. Through numerical simulation, without including the $e+H_2 \rightarrow 2e+H+H^+$ reaction, in the reaction $e+H \rightarrow H+e$, the simulation results are exactly the same. It can be concluded that the author's theoretical analysis about excluding the $e+H \rightarrow H+e$ reaction is reasonable.

3.5 *The anions*

The formation of anion in gas discharge has great significance in the plasma-correlated reactions process. In some gases, atoms or molecules are easily 'attached' by the electrons to form anions. The formation of anion can reduce electrons in the gas, thereby improving the breakdown strength of the gas. Judging from the atomic structure, when the atomic outermost electron is not full, it is easy for the electron to adsorb on the atom to form an anion. Although the working gas – hydrogen – in the cold cathode electric vacuum device can easily adsorb an electron and form anion, it requires the electron energy to reach or exceed 40 eV. But for the low-pressure weakly-ionized plasma, the electron energy cannot reach this value. So anions such as H_2^- cannot form [13]. Therefore, we do not consider anions in the cold cathode electric vacuum device study.

4. Comparison of testing and simulation results

Based on the relevant equations, all the simulations were done by COMSOL, which under the conditions of those 11 types of reactions, exist at the same time. Finally, the potential distributions near the control grid is drawn.

Figure 10 is the simulation curve of the electrical potential near the control grid. The horizontal axis is the time axis, the vertical axis is the potential by which the diffusive current is generated. Figure 11 is the test curve which shows potential changes with time during preionization. The horizontal axis is time and the vertical axis is the potential.

Trigger happens usually in a very short time in experiment (about hundreds of nanoseconds), corresponding to the diffusion current before $1e-7s$ in simulation results. Figure 10 shows that when maximum potential is reached in the internal system, the potential drops rapidly, reaching gradually to a stable value. It is considered that the high potential

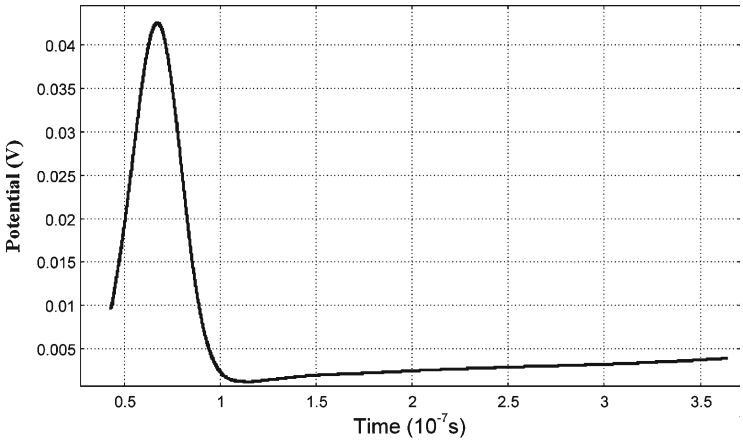

Figure 10. Simulation about potential with time distribution.

before 1e − 7s is due to the collision ionization in cold cathode electric vacuum device. It is mainly by the secondary electrons that the ions collide with cathode resulting in collision ionization reactions between electrons and ions, and therefore it generates current that is mainly due to diffusion. We can see from figure 10, that between 8e − 8s and 1e − 7s, potential inflection point appears. This change is mainly due to the current that is generated by electron diffusion. As time goes on, electrons and ions reach a balance state, finally completing the preionization process.

Simulation results are the calculated voltage with the continuous time function. The test curve is the voltage distribution over time by single pulse. So the voltage drop is slightly different at stable interval after the inflection point appears. Even now, comparing figures 10 and 11, the potential with time relationship of simulation in the preionization process is basically the same with the test relation curves. It can be confirmed

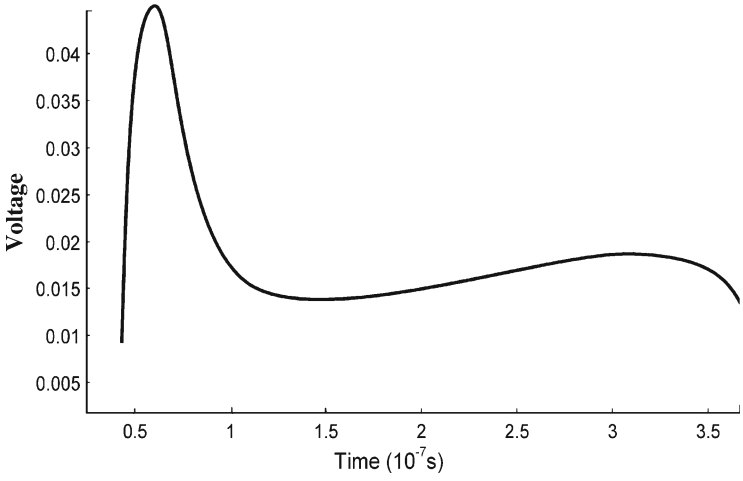

Figure 11. Test image showing voltage changes with time during preionization.

that the reaction type trade-offs of the model in this paper and the settings of the boundary conditions are reasonable.

5. Conclusion

Normally there are 21 types of collision reactions in hydrogen plasma and through theoretical analysis, it is found that in the cold cathode electric vacuum device under low pressure and weak ionization, only 11 types of the inelastic collision reactions out of the 21 reactions are the main reactions that generate plasma in the gas discharge process. The simulation result by considering these 11 reactions have fitted well with the experimental results. These are: four excitation reactions by numerical simulation, four de-excitation reactions, a kind of ionization reaction and two types of surface attachment reactions (totally 11 types of reactions). It is mainly a reaction of gas discharge at low pressure and weak ionization in cold cathode electric vacuum device. At the same time it can also be confirmed that, numerical simulation using finite element method is the effective way to design and optimize electric vacuum device.

Acknowledgements

The authors are grateful to National Natural Science Foundation of China (NNSF, 50877003) for financial support.

References

[1] P Hartmann, H Matsuo, Y Ohtsuka, M Fukao, M Kando and Z Donko, *J. Appl. Phys.* **42**, 3633 (2003)
[2] A Bogaerts and R Gijbels, *Phys. Rev.* **A52**, 5 (1995)
[3] T Kubota, Y Morisaki, A Doughty and J E Lawler, *J. Phys.* **D25**, 613 (1992)
[4] K De Bleecker, D Herrebout, A Bogaerts, R Gijbels and P Descamps, *J. Phys. D: Appl. Phys.* **36**, 1826 (2003)
[5] Michael A Lieberman and Allan J Lichtenberg, *Principles of plasma discharges and materials processing*, 2nd edn (Wiley-Interscience, USA, 2005)
[6] Jung-Sik Yoon, Mi-Yong Song, Jeong-Min Han, Sung Ha Hwang, Won-Seok Chang and BongJu Lee Yukikazu Itikawa, *J. Phys. Chen. Ref. Data* **37**, 2 (2008)
[7] H Tawara, Y Itikawa, H Nishimura and M Yoshino, *J. Phys. Chen. Ref. Data* **19**, 3 (1990)
[8] A V Phelps, *J. Phys. Chen. Ref. Data* **19**, 3 (1990)
[9] Jia-Kou Wang, Wei-Dong Wu, Wei-Guo Sun, Hong-Yan Deng, Xin-Lu Cheng and Yong-Jian Tang, *High Power Laser and Particle Beams* **17**, 10 (2005)
[10] Jin-Chang Pei, *Dyeing and Finishing* **12**, 38 (2005)
[11] Yu-Wen Zhang, Wei-Zhong Ding, Shu-Qiang Guo and Kuang-Di Xu, *Chin. J. Nonferrous Metals* **14**, 2 (2004)
[12] R Celiberto, R K Janev, A Laricchiuta, M Capitelli, J M Wadehra and D E Atems, *At. Data Nucl. Data Tables* **77**, 2 (2001)
[13] Yu-Wen Zhang, *Basic research on reduction of metal oxides with cold plasma hydrogen* (University of Shang Hai, 2005)
[14] R K Janev, D Reiter and U Samm, www.eirene.de/report_4105.pdf
[15] Jun-Ji Yang, *Gas discharge* (Science Press, Beijing, 1983)